Available online at www.sciencedirect.com
ScienceDirect
Journal of Catalysis 245 (2007) 228–236
JOURNAL OF CATALYSIS
www.elsevier.com/locate/jcat

Revealing regioselectivity in hydrogenation of 1-phenyl-1,2-propanedione on Pt catalysts

Ville Nieminen [a,*], Antti Taskinen [b], Matti Hotokka [b], Dmitry Yu. Murzin [a]

[a] *Laboratory of Industrial Chemistry, Process Chemistry Centre, Åbo Akademi University, FIN-20500, Turku/Åbo, Finland*
[b] *Department of Physical Chemistry, Åbo Akademi University, FIN-20500, Turku/Åbo, Finland*

Received 30 June 2006; revised 6 October 2006; accepted 6 October 2006

Abstract

Adsorption of 1-phenyl-1,2-propanedione (**A**), a widely studied molecule in heterogeneously catalyzed enantioselective hydrogenation, and 2,3-hexanedione on a Pt(111) surface was studied using density functional theory. A cluster consisting of two slabs and 31 Pt atoms was used as a model for the catalyst. The results revealed the origin of observed regioselectivity in the hydrogenation of carbonyl groups C1=O1 and C2=O2 of **A** and the lack of regioselectivity in the case of 2,3-hexanedione on Pt catalysts. The adsorption modes of **A** in which the C1=O1 carbonyl group next to the phenyl ring is activated toward hydrogenation ($\eta^2_{C1=O1}$ adsorptions) are more stable than the corresponding adsorption modes where the C2=O2 group is activated ($\eta^2_{C2=O2}$ adsorption). This indicates that the catalyst surface is covered mainly by reaction intermediates leading to the hydrogenation of the carbonyl group C1=O1 and eventually regioselectivity, presuming that the hydrogenation rates of C1=O1 and C2=O2 are of the same order of magnitude. The adsorption energy of 2,3-hexanedione does not depend on which of the carbonyl groups is adsorbed as η^2-mode, and thus the hydrogenation on Pt is not regioselective, as has been observed experimentally. Thus the regioselectivity in the hydrogenation of **A** and 2,3-hexanedione can be explained by the interactions between the substrate and the metal surface.

Keywords: Density functional theory; DFT; Pt; Cluster; Adsorption; Ketone

1. Introduction

Cinchona alkaloid-modified Pt catalysts (active in the Orito reaction [1]) are well known and yet actively investigated examples of heterogeneous enantioselective hydrogenation of the carbonyl group. It has been widely studied, with the main research focus on the mechanistic understanding of enantiodifferentiation on chirally modified Pt (see, e.g., [2,3] and references therein). Enantioselective hydrogenation of 1-phenyl-1,2-propanedione (**A**) has been extensively investigated [4]. The molecule has two reactive carbonyl groups that can be hydrogenated on a chirally modified Pt. The main hydrogenation product of **A**, (*R*)-1-hydroxy-1-phenyl-2-propanone, is an important intermediate in pharmaceutical synthesis, particularly in the production of ephedrine derivatives [5]. This and other (byproduct) hydroxyketones formed can be further hydrogenated enantioselectively to diols [6]. The specific feature of many complex organic molecules is that they have several functional groups that adsorb differently on the catalyst surface and give a wide variety of products. The mode of adsorption is in some cases detrimental or beneficial for the selectivity toward a particular product [7]. Due to the two carbonyl groups in **A**, its hydrogenation has observed to be both regioselective and enantioselective (see Fig. 1); 1-hydroxy products (from the hydrogenation of the C1=O1 group adjacent to the phenyl ring) are formed in excess to 2-hydroxy products (from the hydrogenation of the C2=O2 group next to the methyl group) [8]. Regioselectivity in this context is understood as the preferable reduction of one of the two carbonyl groups; however, in the hydrogenation of 2,3-hexanedione, equal amounts of both carbonyl groups are hydrogenated [9] and no regioselectivity is observed.

* Corresponding author.
E-mail address: ville.nieminen@abo.fi (V. Nieminen).

0021-9517/$ – see front matter
doi:10.1016/j.jcat.2006.10.013

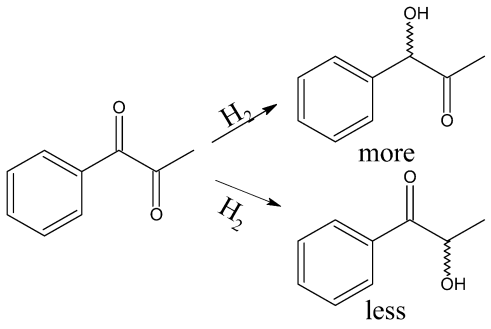

Fig. 1. Illustration of the regioselectivity in the hydrogenation of 1-phenyl-1,2-propanedione on Pt catalyst. 1-OH products are formed in excess [8].

Keeping in mind the industrial applications of the products, the maximization of the yield of the desired product includes both the maximization of enantioselectivity and regioselectivity, and thus the regioselectivity should not be neglected even if the main focus is often on enantioselectivity. It has been observed that in the hydrogenation of **A**, in the absence of the modifier (i.e., nonmodified hydrogenation), the regiomeric ratio (rr, molar ratio of the products that have hydroxyl group adjacent to the phenyl ring and the products that have hydroxyl group adjacent to the methyl group, rr = [1-OH]/[2-OH], also called regioselectivity [9]) is around 4 on Pt/Al_2O_3 catalyst, but it is increased with increasing modifier concentration to a maximum (rr of 10) around a 1:1 surface Pt-to-modifier ratio, after which it gradually starts to decrease [8]. The most interesting observation is the greater than twofold enhancement of rr due to the introduction of small amounts of the modifier. The regioselectivity has been speculated to originate from a longer bond and weaker C=O bond strength at the position 1 of isolated molecule [8], but this observation cannot explain the increased regioselectivity in the presence of the modifier. Although the substrate–modifier interactions are rather well understood [2,10–13] in enantioselective hydrogenation, further understanding is needed with respect to the substrate–catalyst interactions to reveal the regioselectivity.

Recent progress in computational methods has led to a detailed understanding of the substrate–catalyst interactions. Using density functional theory (DFT) and spectroscopic methods the adsorption geometries and energies of benzene, acetone, and acetophenone on Pt(111) have been explored in detail (see, e.g., [14–20] and references therein). It is notable that the DFT calculations can predict the adsorption energies very close to the values obtained experimentally. The aforementioned molecules have functional groups similar to **A** (aromatic and carbonyl moieties), thus a short survey of their adsorption on Pt(111) surface is helpful to understand the adsorption of **A** on a platinum catalyst. Two minimum adsorption energy geometries have been found for benzene on the Pt(111) surface at low coverage: so-called bridge(30) and hollow(0) (see Fig. 2) [14]. The DFT-calculated adsorption energies are in reasonable agreement with the experimental heats of adsorption [14]. In both minimum energy structures, the benzene ring lies parallel to the surface and is distorted with respect to the gas-phase molecule. (For space considerations, we direct the interested reader to the work by Sayes et al. [14] for further details.) Acetone has two main adsorption modes on Pt(111), the so-called η^1- (or end-on) and η^2-adsorption modes [15,16]. In the former, acetone is adsorbed on a surface Pt atom via the oxygen, and two methyl hydrogens also interact with the surface. In the latter, acetone is adsorbed parallel to the surface with some distortion in the structure; a rehybridization of the carbonyl carbon from sp^2 to sp^3 and a considerably longer C=O bond distance than in the gas-phase molecule are observed. The η^2-adsorption mode also has been referred to as an activated species toward hydrogenation and thus, a reaction intermediate [15]. The adsorption of acetophenone is somewhat a combination of the adsorptions of benzene and acetone; the most stable adsorption mode is a combination of the bridge(30) adsorption mode of benzene and the η^2-adsorption mode of acetone [15]. However, adsorption of **A** on Pt(111) surface is more complicated than that of acetophenone, because there is another C=O group that can also interact with the surface.

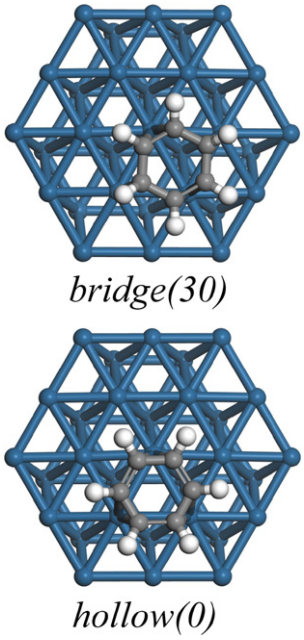

Fig. 2. Illustration of the two most stable adsorption modes of benzene on a Pt31 cluster with a (111) surface.

Here we present a density functional study on the adsorption of 1-phenyl-1,2-propanedione and 2,3-hexanedione on a platinum cluster consisting of 31 atoms and (111) surface. The results are compared with the experimentally observed regioselectivity in the hydrogenation of 1-phenyl-1,2-propanedione and 2,3-hexanedione on nonmodified and modified Pt catalysts.

2. Computational methods

The adsorption complexes of 1-phenyl-1,2-propanedione and 2,3-hexanedione with platinum were studied computationally using the cluster model approach. All calculations were performed using the TURBOMOLE program package [21–23] and DFT with the BP-86 exchange-correlation functional [24–26] in combination with the resolution of the identity (RI) technique (i.e., the total density is approximated,

which allows for a very efficient treatment of Coulomb interactions) [27], as implemented in the TURBOMOLE program package. Note that the BP-86 functional has previously been successfully used to study the adsorption of benzene on Pt(111) [14]. Relativistic effects were taken into account implicitly by using relativistic effective core potential (ECP) from the TURBOMOLE library (def-ecp) to represent the 60 core electrons of Pt. The 18 valence electrons of platinum and all electrons of the other elements were treated explicitly using the SV(P) basis set [def-SV(P)].

A cluster consisting of 31 Pt atoms and two layers with the (111) surface was used to model the catalyst surface. The distances between the Pt atoms were fixed to the bulk value of 277.5 pm, and the seven middle atoms were allowed to fully relax on the top layer. Some calculations were done also for a rigid cluster, that is, where all Pt atoms were fixed. All calculations were done spin unrestricted with the spin state 3 (minimum energy spin state for Pt31 between the states 0 and 10). This choice is respected even if in some cases the minimum electronic state of the bare cluster and/or cluster plus adsorbate is different than 3. A low-spin state should be chosen to represent the electronic structure of a nonmagnetic metal surface (as Pt); it is customary to use the lowest-energy low-spin electronic state for the naked cluster, as well as for the cluster plus its corresponding adsorbate [28]. Furthermore, the spin states are energetically very close to each other, as indicated in Table S1 in the supplementary information. For comparison, some adsorption geometries for a Pt31 cluster having all Pt atoms frozen (rigid cluster) were calculated with a spin state 4, the lowest-energy spin state with a spin below 5 (see Table S1). Test calculations with benzene proved that the adsorption energy changed very little when the spin state was changed; the adsorption energies for the bridge(30) adsorption mode were -124 kJ mol^{-1} for spin state 3 and -122 kJ mol^{-1} for spin states 4 and 5. For a rigid cluster, the corresponding adsorption energies were -88 ($S = 4$) and -86 kJ mol^{-1} ($S = 8$). Similarly, the adsorption energy for the fcc-hollow(0) site was -75 kJ mol^{-1} (-48 kJ mol^{-1} for a rigid cluster). As can be seen, the adsorption energies are in accordance with the experimental TPD results for two different adsorption sites with adsorption enthalpies of -117 to -129 for lower coverage [representing the bridge(30) adsorption mode] and -82 to -86 kJ mol^{-1} for higher coverage [representing the hollow(0) adsorption mode] [29,30]. The calculations with the triple-ζ valence plus polarization (TZVP) basis set gave similar results as the calculations with the SV(P) basis set; changes in the adsorption geometry of benzene via the bridge(30) mode on Pt31 were negligible, and the adsorption energy was -119 kJ mol^{-1} with the basis set superposition error of 56 kJ mol^{-1}.

2.1. BSSE

The SV(P) basis set together with the effective core potentials is rather incomplete, giving rise to a basis set superposition error (BSSE) of 60.0 kJ mol^{-1} for the bridge(30) mode of benzene adsorbed on a Pt31 cluster. This BSSE is comparable to 65.9 kJ mol^{-1} from the previous calculations using a double-ζ basis set [14]. Note, however, that according to our cluster model calculations, the energy difference between the bridge(30) and hollow(0) adsorption modes of benzene, 49 kJ mol^{-1} (40 kJ mol^{-1} for a rigid cluster), is in reasonable agreement with the experimental results; the difference between the adsorption enthalpies is 31–47 kJ mol^{-1}. This observation provided justification for using the SV(P) basis set throughout this study, because increasing the basis set (to, e.g., TZVP) would have increased the computational effort considerably without any significant change in the geometry, adsorption energy, or decrease in the BSSE. Furthermore, the calculated adsorption energies (both absolute values and difference between the adsorption modes) are very close to those obtained experimentally. This is in line with the observation of Masamura, who studied interaction energies of ion–water cluster and observed that with the aug-cc-pVDZ basis set, the counterpoise-uncorrected intermolecular interaction energies are more reliable than the corresponding counterpoise-corrected energies [31]. In addition, we want to stress that the counterpoise method always overestimates the BSSE, and there is no clear way to correct for this overestimation [32]. The role of the BSSE is rather negligible from a catalysis standpoint; we are interested mainly in the energy differences, and the BSSE tends to cancel for these differences rather equally.

3. Results

The numbering of the atoms and relevant torsion angles of **A** and 2,3-hexanedione are shown in Fig. 3. The adsorption energies and geometrical details of the adsorption complexes are given in Table 1, and the adsorption geometries are illustrated in Figs. 4–7. Several adsorption geometries with different adsorption modes for the molecules were optimized. Note that there exist several minima for each adsorption mode on the potential energy surface (PES), and finding the geometry corresponding to the global minimum can be tricky. Only the most stable structure of each adsorption mode found has been reported in this paper; the following criteria were used to find them. First, two possible conformations of the molecules were considered, that is, s-*cis* and s-*trans* conformations, where the carbonyl oxygens are on the same (Fig. 5) and opposite (Fig. 4) sides of the C1–C2

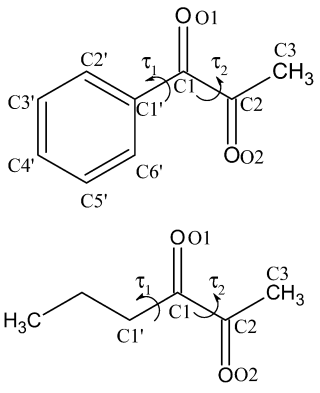

Fig. 3. Numbering of atoms and definitions of torsion angles τ_1 and τ_2 of 1-phenyl-1,2-propanedione and 2,3-hexanedione.

Table 1
Adsorption energies, bond distances and relevant angles for different adsorption modes of 1-phenyl-1,2-propanedione. For the numbering of the atoms, see Fig. 3

Adsorption mode[a]	ΔE_{ads}[b] (kJ mol^{-1})	C1=O1 (pm)	C2=O2 (pm)	C–Pt[c] (pm)	O–Pt[c] (pm)	τ_1 (°)	τ_2 (°)	φ_1[d] (°)	φ_2[e] (°)	C1′–C1 (pm)
s-*trans* $\eta^2_{C1=O1}$	−169 (−109)	133	123	223	216	45	156	143	177	152
s-*trans* bridge(30)	−129 (−93)	124	126	289	225	22	164	167	170	153
s-*trans* $\eta^2_{C2=O2}$	−111 (−72)	123	135	221	211	20	152	178	137	153
s-*trans* hollow(0)	−104 (−53)	122	135	221	213	20	145	178	136	153
s-*cis* $\eta^2_{C1=O1}$	−135	133	122	223	213	7	22	145	179	153
s-*cis* bridge(30)	−89 (−50)	124	123	275[f]	324[g]	15	56	165	168	153
s-*cis* hollow(0)	−44 (−18)	128	122	264	281	17	4	162	176	152
s-*cis* $\eta^2_{C2=O2}$	−38 (−30)	126	135	224	208[h]	−39	30	172	132	149
s-*trans* η^1_{O1}	−19	124	122	–	271	19	135	180	176	149
s-*cis* $\eta^1_{O1,O2}$	−3	126	125	–	220[i]	40	−15	172	177	149
A (isolated)	–	123	122	–	–	2	155	179	177	150

[a] Subscript indicates the atom(s) in contact with the Pt surface.
[b] ΔE_{ads} on a rigid cluster are given in the parentheses.
[c] The closest C and O atoms to the surface Pt, typically the ones that are η^2 adsorbed.
[d] Indicates distortion from planarity, $\varphi_1 = \angle(C1', C1, C2, O1)$.
[e] Indicates distortion from planarity, $\varphi_2 = \angle(C1, C2, C3, O2)$.
[f] For C1.
[g] For O1, 326 pm for O2.
[h] 223 pm for O1.
[i] For O1, 219 pm for O2.

bond, respectively. Second, the two most stable adsorption modes found for benzene [14], the bridge(30) and hollow(0) modes, were studied; these should give the most stable adsorption modes for the aromatic moiety of **A**. Third, adsorption of the C=O moiety at positions 1 (C1=O1) or 2 (C2=O2) in a so-called η^2-mode (see the $\eta^2_{C1=1}$ and $\eta^2_{C2=O2}$ structures in Figs. 4 and 5) was studied, because this mode is considered the relevant one for hydrogenation [15]. For comparison, two purely spectator species—end-on or η^1-adsorption modes for the s-*cis* and s-*trans* conformations—were optimized (Fig. 6). As in the case of acetone and acetophenone, the η^2-adsorption mode is essential for hydrogenation, because it is considered the activated one toward hydrogenation due to rehybridization of the carbonyl carbon and increased C=O bond distance [15]. The reaction (hydrogenation) rate depends on the proportion between activated and spectator species on the catalyst surface [15]. In the present study, we concentrate on the comparison between the modes where the C1=O1 and C2=O2 carbonyl groups are activated (i.e., the $\eta^2_{C1=O1}$- and $\eta^2_{C2=O2}$-adsorption modes). Altogether, 10 different adsorption modes were studied. For 2,3-hexanedione, only the η^2-adsorption modes for both carbonyl groups were considered.

3.1. s-trans conformation of *A*

In all s-*trans* structures, the aromatic moiety was chemisorbed on the surface (Fig. 4). The bond distance from phenyl carbon C1′ to C1 was increased by 2–3 pm compared with the isolated molecule, and the C–C distances in the phenyl ring varied from 144 to 149 pm, whereas in the isolated molecule, the C–C bond distances were 140–142 pm. The Pt–C bond distances from Pt surface atoms to the phenyl ring carbons varied mainly between 214 and 235 pm. Note that the torsion angle τ_2 (Fig. 3) in all s-*trans* structures was close to the optimized value for the isolated molecule (155°) varying from 145° to 164°. The adsorption mode s-*trans* $\eta^2_{C1=O1}$ resembled that of acetone; the C=O moiety was also adsorbed on the Pt surface via oxygen and carbon, and the phenyl group was adsorbed in the bridge(30) mode. The C=O bond distance was elongated to 133 pm, and the carbon was rehybridized from sp^2 to close to sp^3. The C–Pt and O–Pt distances were 223 and 216 pm. This structure was the most stable one on the Pt31 cluster, with an adsorption energy of −169 kJ mol^{-1}. The second most stable structure was that in which the aromatic moiety was adsorbed in the bridge(30) mode but the carbonyl moieties did not interact with the surface to a significant extent; the C=O bond distances were just slightly longer (by 2 and 4 pm) than those in the isolated molecule. The adsorption energy of −129 kJ mol^{-1} was close to the corresponding ΔE_{ads} of bridge(30) adsorbed benzene. In both structures in which the phenyl ring was bridge(30) adsorbed, **A** had a nonapical substitution. In the s-*trans* hollow(0) and s-*trans* $\eta^2_{C2=O2}$-adsorption modes of **A**, the carbonyl moiety C2=O2 next to the methyl group was also adsorbed on the surface via the η^2-mode, as demonstrated by the increased C2=O2 bond distances and rehybridization of the carbon C2. Note that the structure of **A** restricted proper adsorption of both C2=O2 and the phenyl ring at the same time. In the $\eta^2_{C2=O2}$-adsorption mode, the aromatic moiety was adsorbed almost at the bridge(0) site but was somewhat distorted; the C–Pt distances were slightly longer in the side where the C2=O2 moiety was adsorbed. The adsorption energies were greater for both $\eta^2_{C2=O2}$ and hollow(0) modes ($\Delta E_{ads} = -111$ and -104 kJ mol^{-1}, respectively) compared with the corresponding benzene adsorption energies (−78 and −75 kJ mol^{-1}, respectively) due to adsorption of both C2=O2 and the aromatic moieties. The adsorption energy of the s-*trans* η^1_{O1}-adsorption mode (Fig. 6) was only −19 kJ mol^{-1}, indicating that the presence of this mode was negligible, at least at low

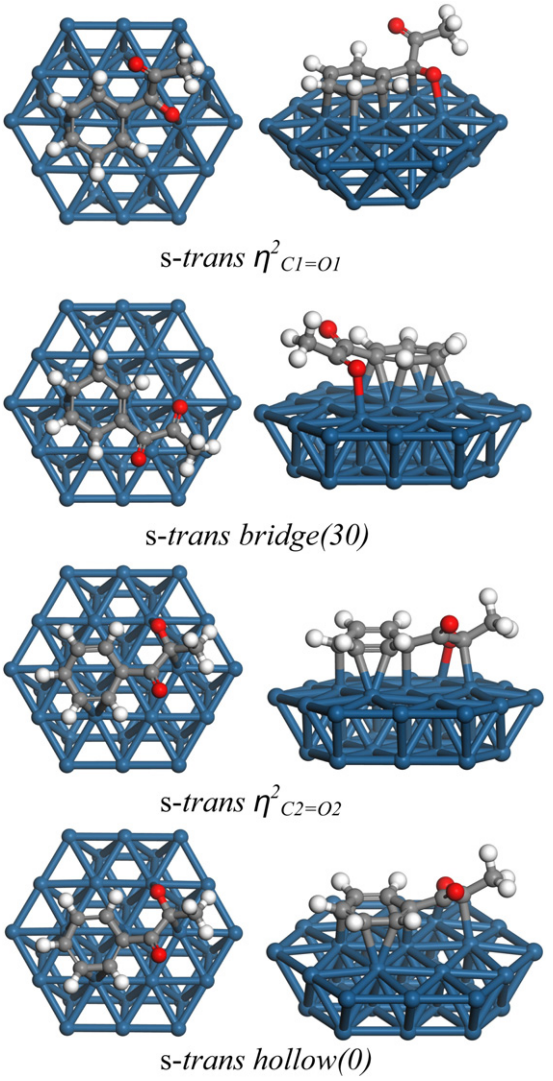

Fig. 4. Illustration of the adsorption modes of 1-phenyl-1,2-propanedione adopting the s-*trans* conformation on the Pt31 cluster from top (left) and side (right).

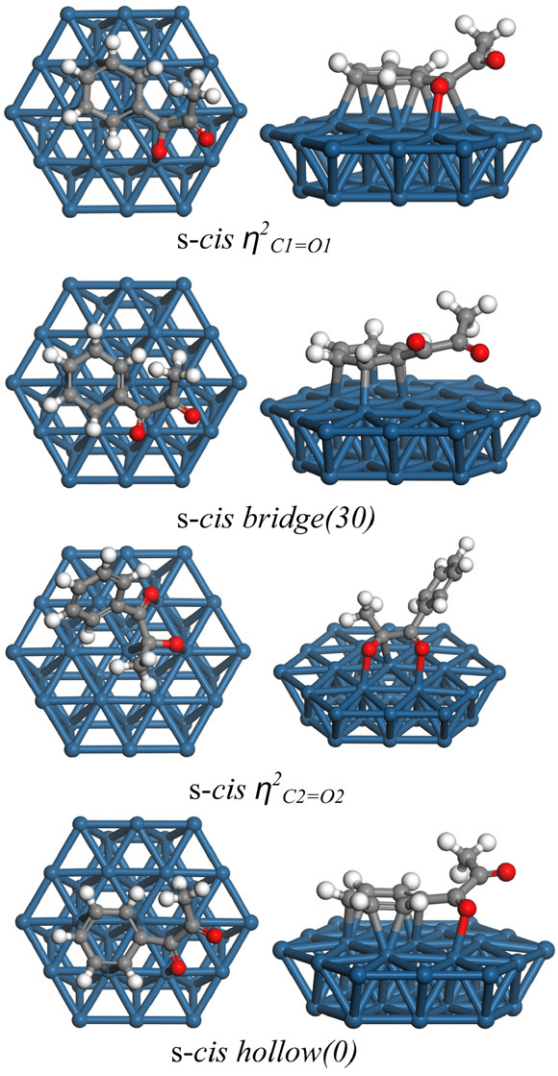

Fig. 5. Illustration of the adsorption modes of 1-phenyl-1,2-propanedione adopting the s-*cis* conformation on the Pt31 cluster from top (left) and side (right).

coverage. The geometry was close to that of the isolated **A**, and O1 interacted with the surface (end-on adsorption), with a Pt–O distance of 271 pm.

3.2. *s-cis conformation of* ***A***

It is notable that no stable s-*cis* conformation was found on the PES of the isolated **A** molecule. However, the Pt(111) surface imposed a steric restriction, leading to a stable s-*cis* conformation on the surface. The close contact and interaction between the two oxygens of **A** led to destabilization of the adsorption modes of s-*cis* conformation, as marked by lower adsorption energies than in the case of s-*trans* conformation. In the adsorption modes of s-*cis* conformation, both C=O groups were on the same side of the C1–C2 bond, with the torsion angle τ_2 varying between 20° and 45° (Fig. 5). In the adsorption mode where the C1=O1 moiety was activated (i.e., s-*cis* $\eta^2_{C1=O1}$), the C=O moiety was adsorbed on the Pt surface via oxygen and carbon, and the phenyl group was adsorbed in the bridge(30) mode. This was the most stable s-*cis*-conformation ($\Delta E_{ads} = -135$ kJ mol^{-1}), followed by bridge(30) ($\Delta E_{ads} = -89$ kJ mol^{-1}), in which only the phenyl group was chemisorbed on the surface, but the C=O groups did not interact with the Pt to a large extent. In the adsorption mode where the C2=O2 moiety was activated (i.e., s-*cis* $\eta^2_{C2=O2}$), the phenyl ring was not chemisorbed on the surface, leading to a rather low adsorption energy of -38 kJ mol^{-1}. Simultaneous chemisorption of the C2=O2 and phenyl moieties in s-*cis* $\eta^2_{C2=O2}$ was practically impossible due to the sp^2 hybridization of the C1 carbon next to the phenyl ring. Attempts to find such a geometry always led to another adsorption mode, for instance, to s-*cis* $\eta^2_{C1=O1}$. In the case of the s-*cis* hollow(0) mode, neither of the C=O groups could adsorb on the surface via the η^2-mode, but the carbonyl moiety next to the phenyl group interacted slightly with the surface, and the C1=O1 bond distance was somewhat increased (Table 1). The adsorption energy was less than that for hollow(0) of benzene due to the destabilizing interaction between the oxygens in **A**. The adsorption energy of

s-*cis* $\eta^1_{O1,O2}$-adsorption mode was only -3 kJ mol^{-1}, indicating that it was not present on the surface, at least at low coverage. The geometry differed from that of the isolated **A** by the torsion angle τ_2, because the s-*cis* conformation was stable due to the interaction of both oxygens with the surface.

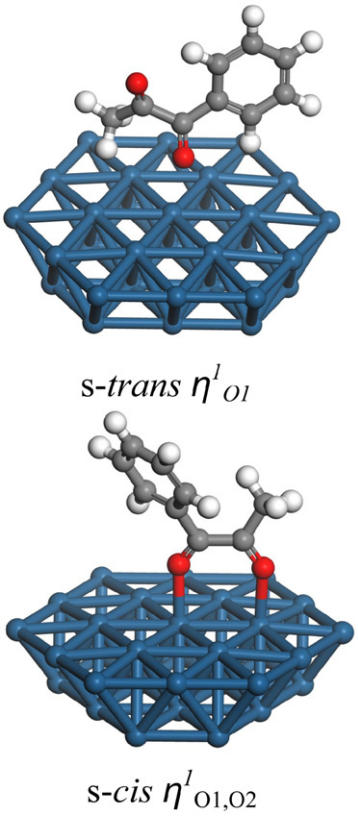

Fig. 6. Illustration of the η^1-adsorption modes of 1-phenyl-1,2-propanedione adopting the s-*cis* and s-*trans* conformations on the Pt31 cluster.

3.3. 2,3-Hexanedione

The η^2-adsorption modes of 2,3-hexanedione via C=O moieties at positions 1 and 2 (see the numbering in Fig. 3) are shown in Fig. 7. The adsorption energies for the s-*trans* η^2-modes were almost equal (-36 kJ mol^{-1} for $\eta^2_{C2=O2}$ and -33 kJ mol^{-1} for $\eta^2_{C1=O1}$) even if there were minor differences in the conformations between the adsorption modes. The difference in ΔE_{ads}, 3 kJ mol^{-1}, was below the level of accuracy that can be obtained by these DFT calculations. The bond distances (in pm: adsorbed C=O 133/134; nonadsorbed C=O 122; C–Pt 225/224; O–Pt 213/212) were comparable to those obtained for η^2-adsorption of **A**. The adsorption energies of s-*cis* η^2 were also equal (-39 kJ mol^{-1} for $\eta^2_{C2=O2}$ and -38 kJ mol^{-1} for $\eta^2_{C1=O1}$), and the bond distances were comparable to those mentioned above. The slightly higher adsorption energies of the s-*cis* η^2-adsorption modes were due to the interaction between the C=O group that was not activated and the Pt surface not present in the s-*trans* η^2-adsorption modes. This interaction energy apparently overcame the destabilizing effect of two adjacent oxygens repelling each other. Spectator species (i.e., η^1-adsorption modes of 2,3-hexanedione) were not considered in this study, because they are not relevant for hydrogenation.

4. Discussion

4.1. Active species toward hydrogenation

Two proposals on the nature of activated species in acetone hydrogenation have been addressed in the literature. Vargas et al. suggested that η^2-adsorbed acetone is a reaction intermediate preceding the hydrogenation step [15]. This is understandable, because in the η^2-adsorption geometry of acetone, the carbonyl C is significantly rehybridized similar to the carbons

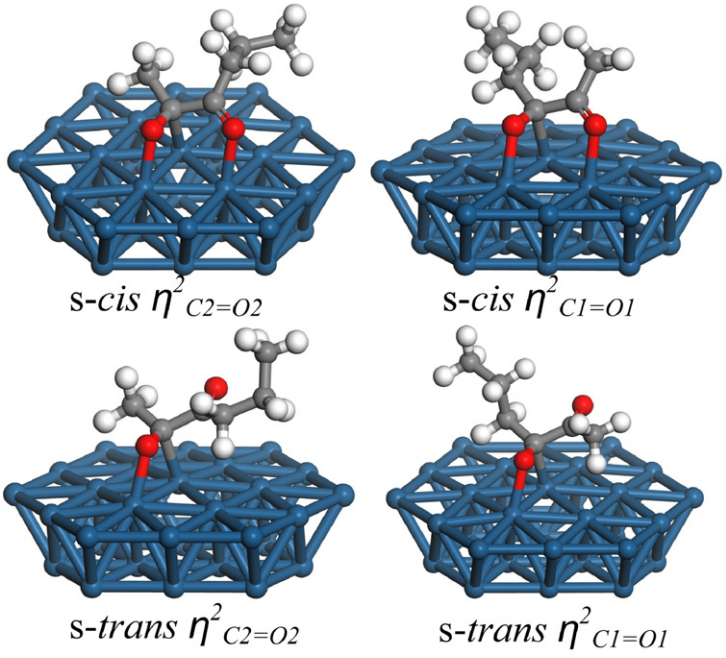

Fig. 7. Illustration of the η^2-adsorption modes of 2,3-hexanedione in s-*cis* and s-*trans* conformations on the Pt31 cluster.

in the di-σ adsorption of ethylene on Pd. Transition-state calculations have shown that this rehybridized di-σ adsorption state of ethylene is the active one for the successive hydrogenation step [33]. Note that the di-σ adsorption of ethene on Pt is essentially the same as that on Pd [34]. For ketones, in analogy with ethylene, the rehybridization can be viewed as a step toward the formation of hydrogenated species [15]. Jeffery et al. proposed that in the case of acetone, another species observed in the surface science experiments besides the η^1-adsorbed acetone is the so-called μ_2(C1, O) enolate [16]; moreover, the second species is not likely to be a ketone adsorbed parallel to the surface (i.e., η^2 acetone). This would suggest that enol and enolate species are present on the Pt surface during hydrogenation of ketones for which keto enol isomerization is possible. In fact, it has been shown that the hydrogenation of methyl pyruvate (an alpha-keto ester) occurs via the enol isomer of the reactant on the Pd surface [35]. It is notable that a similar mechanism has not been observed in the corresponding reactions over Pt [16]; however, in the case of **A**, the role of the enol forms is negligible. It has been shown that hydrogenation of **A** over Pd (and Pt) does not proceed via an enol form [36]. Furthermore, an enol form only of a carbonyl group C2=O2 can be formed (compare the structure of **A** in Fig. 1 to that of acetone); this will lead to the formation of a 2-OH product that is actually formed to a minor extent, contradicting the possibility that the enol forms play a significant role in the hydrogenation of **A**. Summarizing, in the current study, the structures in which C=O is η^2 adsorbed on the Pt surface are considered to be the only active species. In general, Diezi et al. have proposed that in the case of 1,1,1-trifluoro-2,4-diketones, the η^2-adsorbed enol forms can be the reactive species in the hydrogenation of the activated ketone on chirally modified Pt [37].

4.2. Active and spectator species

We now consider the adsorption geometries and energies in their relation to the hydrogenation of **A**. The most stable structure found on the PES is that in which the phenyl ring was adsorbed via the bridge(30) mode and the C1=O1 carbonyl group was also adsorbed via the η^2-mode. This structure was 34 kJ mol^{-1} more stable than the second most stable structure, s-*cis* $\eta^2_{C1=O1}$. In both structures, the C1=O1 carbonyl group next to the phenyl ring was activated toward hydrogenation; the carbon was rehybridized, and the C1=O1 bond was considerably elongated. The adsorption energies of these two structures were considerably larger than those of the structures, where the carbonyl moiety C2=O2 next to the methyl group was activated. The s-*trans* and s-*cis* $\eta^2_{C2=O2}$ structures had adsorption energies of -111 and -38 kJ mol^{-1}, compared with the s-*trans* and s-*cis* $\eta^2_{C1=O1}$ structures' adsorption energies of -169 and -135 kJ mol^{-1}. It is noteworthy that the carbonyl group C2=O2 was also activated in the s-*trans* hollow(0) adsorption mode, resulting in a higher adsorption energy than that for benzene's hollow(0) adsorption. Therefore, this species is not considered a spectator species. In the other adsorption modes, neither carbonyl group was significantly activated, because the C=O bond was not elongated or just slightly elongated to 124–128 pm. When the C=O was completely activated, the bond distance was as long as 133 pm. Thus, we consider the adsorption modes in which neither of the carbonyl groups was not completely activated as spectator species in the hydrogenation reaction or as intermediates leading to activated species, when the C=O double bond was partly activated. The amount of the spectator species on the surface did not seem to be high at low coverage, as can be seen from the adsorption energies; the most stable spectator species s-*trans* bridge(30) had $\Delta E_{ads} = -129$ kJ mol^{-1}, being less stable than that of both the s-*trans* and s-*cis* $\eta^2_{C1=O1}$ modes. The s-*trans* bridge(30) adsorption mode could switch to s-*trans* $\eta^2_{C1=O1}$ by turning 30° on the surface having a bridge(0) adsorption mode for the phenyl ring as an intermediate step.

We have considered three spectator species with aromatic moiety chemisorbed on the surface: s-*trans* bridge(30), s-*cis* bridge(30), and s-*cis* hollow(0). The adsorption modes with one C=O group activated (η^2-adsorbed) are considered activated toward hydrogenation and reaction intermediates. The real spectator species, s-*cis* and s-*trans* η^1 adsorbed **A**, in which aromatic moiety was not chemisorbed on the surface, did not play a major role in the hydrogenation reaction; their concentration on the Pt(111) surface was rather low (at least at low coverage) as can be seen in the adsorption energies -19 (s-*trans* η^1_{O1}) and -3 kJ mol^{-1} (s-*cis* $\eta^1_{O1,O2}$).

4.3. Hydrogenation of *A* and 2,3-hexanedione on Pt

We now consider the racemic hydrogenation of **A** on Pt catalyst without any modifier, such as cinchonidine preadsorbed on the Pt surface by comparing our results with those of the adsorption and reactivity of acetone. In the case of acetone hydrogenation, Vargas et al. reported that the nonactivated spectator species with the η^1-adsorption mode was more stable on the Pt(111) surface than the η^2-adsorption mode, leading to greater coverage of the nonactivated species; thus, the reaction was slow (59% for acetone after 2 h over Pt catalyst) [15]. However, on substituting one methyl group's hydrogen atoms with fluorine atoms, the two adsorption modes become almost equal in stability. This is the probable reason for the higher hydrogenation rate of trifluoroacetone compared with acetone [15]. In other words, larger proportion of the activated adsorbed intermediates would lead to a higher hydrogenation rate. If we apply a similar analysis to the adsorption of **A**, we find that the hydrogenation rates of the two carbonyl groups (i.e., the regioselectivity) depend on the ratio (that is proportional to the adsorption energy) of the adsorption mode(s), in which the reacting carbonyl group is activated (η^2-adsorbed C1=O1 and C2=O2). Now the regioselectivity in the hydrogenation of **A** is understandable. The adsorption energy and thus the coverage are higher for the η^2-adsorption modes of C1=O1 than for C2=O2 (Table 1), leading to a higher hydrogenation rate of C1=O1. In the foregoing analysis, we assumed that the hydrogenation rates for both carbonyl groups were of the same order of magnitude and thus the reaction was under thermodynamic control. In the case of kinetic control, the hydrogenation rate of C2=O2 could be higher than C1=O1 (or vice versa),

also leading to regioselectivity. However, the chemical environment of both the carbonyl moieties was rather similar; only one substituent was different (methyl vs phenyl). The phenyl group next to the hydrogenated carbonyl group likely had only a minor effect on the reaction rate compared with the methyl group by decreasing the activation barrier, because the C1=O1 bond was just slightly weaker than the C2=O2 bond [8]. Comparing the adsorption energies of 2,3-hexanedione clearly shows why no regioselectivity occurs in its hydrogenation [9]; the adsorption energies for the s-*cis* and s-*trans* conformations of the $\eta^2_{C1=O1}$- and $\eta^2_{C2=O2}$-adsorption modes were equal, and thus equal amounts of activated C1=O1 and C2=O2 species existed on the Pt surface. Thus, neither of the hydrogenation products 2-hydroxy-3-hexanone or 3-hydroxy-2-hexanone was formed in excess. This is also in accordance with the experimental findings and supports the conclusions reached for **A**. Note that the adsorption of hydrogen is not taken into account in these calculations. However, it is reasonable to assume that the effect of the co-adsorbed hydrogen on the adsorption energies would be almost the same for both $\eta^2_{C1=O1}$- and $\eta^2_{C2=O2}$-adsorption modes, and thus the difference in the stabilities would also be at the same order of magnitude as discussed above.

The reason for the increased regioselectivity in the presence of a modifier is not clear. It is tempting to speculate that the increase is related to the energy difference of the s-*cis* conformations on the surface. According to the enantioselective hydrogenation model of **A**, it adopts only the s-*cis* conformation while interacting with the modifier [11], and thus the s-*trans* conformations can be neglected. Comparing the adsorption energy values in Table 1 shows that the energy difference (and thus the ratio of their amounts) actually increased between the $\eta^2_{C1=O1}$- and $\eta^2_{C2=O2}$-adsorption modes if only the s-*cis* conformations were considered, indicating higher proportional coverage of the $\eta^2_{C1=O1}$ adsorption mode. However, the calculations in [11] were carried out without the presence of the Pt surface. Diezi et al. [37] pointed out that the fundamental differences in the structures of the substrate–modifier ion pair in solution and on the Pt surface mean that the reaction mechanism cannot be understood without considering the adsorption on the metal surface. Therefore, the reason for the increase in the enantioselectivity remains a topic for future study, in which the metal surface will be explicitly accounted for. Nevertheless, the regioselectivity in the hydrogenation of **A** and 2,3-hexanedione can be correlated with the interactions between the substrate and the nonmodified metal surface by comparing the stabilities of the $\eta^2_{C1=O1}$- and $\eta^2_{C2=O2}$-adsorption modes.

5. Conclusion

Adsorption of two diketones, 1-phenyl-1,2-propanedione (**A**) and 2,3-hexanedione, on a flat Pt(111) surface was studied using density functional theory. A cluster consisting of 31 Pt atoms in two slabs was used as a model for the catalyst. The results revealed the origin of observed regioselectivity in the hydrogenation of **A** (i.e., hydrogenation of C=O group next to the phenyl ring in excess), as well as the reason why no regioselectivity was observed for 2,3-hexanedione on Pt catalysts. The most stable adsorption modes of **A** were those in which both the aromatic moiety and the adjacent carbonyl group were chemisorbed on the surface, namely s-*trans* $\eta^2_{C1=O1}$ and s-*cis* $\eta^2_{C1=O1}$, with adsorption energies of -169 and -135 kJ mol^{-1}. In these adsorption modes, the carbonyl group next to the phenyl ring (C1=O1) was activated and can be considered a reaction intermediate toward hydrogenation. The adsorption energy of the competing group C2=O2 next to the methyl group (i.e., s-*trans* $\eta^2_{C2=O2}$) was much lower, -111 kJ mol^{-1}. This indicates that the nonmodified catalyst surface was covered mainly by reaction intermediates, leading to the hydrogenation of the carbonyl group C1=O1 and eventually regioselectivity, presuming that the hydrogenation rates of C1=O1 and C2=O2 were of the same order of magnitude. In the case of 2,3-hexanedione hydrogenation, η^2 adsorption of both carbonyl groups resulted in equal adsorption energy and thus lack of regioselectivity, as observed experimentally. Thus, the regioselectivity in the hydrogenation of **A** and 2,3-hexanedione can be correlated with the interactions between the substrate and metal surface.

Acknowledgments

This work is part of the activities at the Åbo Akademi Process Chemistry Centre within the Finnish Centre of Excellence Programme (2000–2011) of the Academy of Finland. V.N. thanks the Academy of Finland (project 212620) for financial support. Resources provided by CSC, the Finnish IT Center for Science, are kindly acknowledged.

Supplementary information

A table containing relative energies of different spin states for a Pt31 cluster can be found in the online version of the article.

Please visit doi: 10.1016/j.jcat.2006.10.013.

References

[1] Y. Orito, S. Imai, S. Niwa, J. Chem. Soc. Jpn. 8 (1979) 1118.
[2] T. Bürgi, A. Baiker, Acc. Chem. Res. 37 (2004) 909.
[3] D.Yu. Murzin, P. Mäki-Arvela, E. Toukoniitty, T. Salmi, Catal. Rev. 47 (2005) 175.
[4] E. Toukoniitty, P. Mäki-Arvela, M. Kuzma, A. Villela, A. Kalantar Neyestanaki, T. Salmi, R. Sjöholm, R. Leino, E. Laine, D.Yu. Murzin, J. Catal. 204 (2001) 281.
[5] V.B. Shukla, P.R. Kulkarni, World. J. Microbiol. Biotechnol. 16 (2000) 499.
[6] V. Nieminen, A. Taskinen, E. Toukoniitty, M. Hotokka, D.Yu. Murzin, J. Catal. 237 (2006) 131.
[7] R.J. Berger, E.H. Stitt, G.B. Marin, F. Kapteijn, J.A. Moulijn, CATTECH 5 (2001) 36.
[8] E. Toukoniitty, P. Mäki-Arvela, V. Nieminen, M. Hotokka, J. Päivärinta, T. Salmi, D.Yu. Murzin, Catalysis of Organic Reactions, Decker, New York, 2002, pp. 341–348.
[9] J. Slipszenko, S.P. Griffiths, P. Johnston, K.E. Simons, W.A.H. Vermeer, P.B. Wells, J. Catal. 179 (1998) 267.
[10] A. Vargas, T. Bürgi, M. von Arx, R. Hess, A. Baiker, J. Catal. 209 (2002) 489.
[11] E. Toukoniitty, V. Nieminen, A. Taskinen, J. Päivärinta, M. Hotokka, D.Yu. Murzin, J. Catal. 224 (2004) 326.

[12] A. Taskinen, E. Toukoniitty, V. Nieminen, D.Yu. Murzin, M. Hotokka, Catal. Today 100 (2005) 373.
[13] N. Bonalumi, T. Bürgi, A. Baiker, J. Am. Chem. Soc. 125 (2003) 13342.
[14] M. Sayes, M.-F. Reyniers, G.B. Marin, M. Neurock, J. Phys. Chem. B 106 (2002) 7489.
[15] A. Vargas, T. Bürgi, A. Baiker, J. Catal. 222 (2004) 439.
[16] E.L. Jeffery, R.K. Mann, G.J. Hutchings, S.H. Taylor, D.J. Willock, Catal. Today 105 (2005) 85.
[17] C. Morin, D. Simon, P. Sautet, J. Phys. Chem. B 107 (2003) 2995.
[18] C. Morin, D. Simon, P. Sautet, J. Phys. Chem. B 108 (2004) 5653.
[19] C. Morin, D. Simon, P. Sautet, J. Phys. Chem. B 108 (2004) 12084.
[20] N. Bonalumi, A. Vargas, D. Ferri, A. Baiker, J. Phys. Chem. B 110 (2006) 9956.
[21] R. Ahlrichs, M. Bär, H. Horn, C. Kölmel, Chem. Phys. Lett. 162 (1989) 165.
[22] M. Häser, R. Ahlrichs, J. Comput. Chem. 10 (1989) 104.
[23] M. von Arnim, R. Ahlrichs, J. Comput. Chem. 19 (1998) 1746.
[24] J.P. Perdew, Phys. Rev. B 33 (1986) 8822.
[25] J.P. Perdew, Phys. Rev. B 34 (1986) 7046.
[26] A.D. Becke, J.P. Perdew, Phys. Rev. A 38 (1988) 3098.
[27] K. Eichorn, O. Treutler, H. Öhm, M. Häser, R. Ahlrichs, Chem. Phys. Lett. 240 (1994) 283.
[28] F. Illas, C. Sousa, J.R.B. Gomes, A. Clotet, J.M. Ricart, Theoretical Aspects of Heterogeneous Catalysis, in: M.A.C. Nascimento (Ed.), Progress in Theoretical Chemistry and Physics, vol. 8, 2001, pp. 149–181.
[29] J.M. Campbell, S.G. Seimanides, C.T. Campbell, J. Phys. Chem. 93 (1989) 815.
[30] C. Xu, Y.-L. Tsai, B.E. Koel, J. Phys. Chem. 98 (1994) 585.
[31] M. Masamura, Theor. Chem. Acc. 106 (2001) 301.
[32] C.J. Cramer, Essentials of Computational Chemistry – Theory and Models, Wiley, Chichester, 2002, p. 183.
[33] M. Neurock, R.A. van Santen, J. Phys. Chem. B 104 (2000) 11127.
[34] G.W. Watson, R.K.P. Wells, D.J. Villock, G.J. Hutchings, J. Phys. Chem. B 104 (2004) 6439.
[35] T.J. Hall, P. Johnston, W.A.H. Vermeer, S.R. Watson, P.B. Wells, Stud. Surf. Sci. Catal. 101 (1996) 221.
[36] E. Toukoniitty, S. Franceschini, A. Vaccari, D.Yu. Murzin, Appl. Catal. A Gen. 300 (2006) 147.
[37] S. Diezi, D. Ferri, A. Vargas, T. Mallat, A. Baiker, J. Am. Chem. Soc. 128 (2006) 4048.